Recent results in curvelet-based primary-multiple separation: application to real data

Deli Wang, Jilin University, Rayan Saab, ECE-UBC, Ozgur Yilmaz, Math-UBC and Felix J. Herrmann, EOS-UBC

SUMMARY

In this abstract, we present a nonlinear curvelet-based sparsity-promoting formulation for the primary-multiple separation problem. We show that these coherent signal components can be separated robustly by explicitly exploiting the locality of curvelets in phase space (space-spatial frequency plane) and their ability to compress data volumes that contain wavefronts. This work is an extension of earlier results and the presented algorithms are shown to be stable under noise and moderately erroneous multiple predictions.

INTRODUCTION

In complex areas, multiple suppression techniques based on move-out filtering fail because the assumptions on the hyperbolic move-out in the CMP-offset domain are not met. Furthermore, the occurrence of shallow, high-velocity layers can lead to small move-out differences between primaries and multiples which are difficult to interpret. These complications may result in unsatisfactory separation of primaries and multiples.

In cases where move-out filtering based methods fail, 'wave-equation'-based predictive methods (Verschuur et al., 1992; Fokkema and van den Berg, 1993; Weglein et al., 1997) have shown considerable improvements. Wave-equation methods consist of two main steps: the multiple-prediction and the primary-multiple separation step. The separation step is often referred to as adaptive subtraction, during which imperfections in the predictions, such as the water bottom reflectivity (see e.g. Berryhill and Kim, 1986; Wiggins, 1988; Lokshtanov, 1999) or source and receiver characteristics (Verschuur et al., 1992; Berkhout and Verschuur, 1997; Ikelle et al., 1997), are absorbed by a matched-filtering procedure. This procedure is important because predictions for surface-related multiples as well as internal multiples based on two-dimensional input data (see e.g. Verschuur et al., 1992; Berkhout and Verschuur, 1997; Coates and Weglein, 1996) are often inaccurate in situations where the subsurface displays three-dimensional complexity. Other complications determining the success of multiple attenuation include source-receiver directivity, ghosts and the obliquity factor, unbalanced amplitudes of multiple predictions that consist of mixtures of different-order multiples (Verschuur and Berkhout, 1997; Chen et al., 2004), and incomplete data, e.g., due to missing near offsets, or unequal source and receiver spacing both of which may give rise to artifacts in the predicted multiples (see Verschuur, 2006).

Several attempts have been made to improve multiple elimination by either increasing the accuracy of the multiple predictions or by devising a more robust subtraction/separation methodology. Examples of the first approach are methods based on model-driven time delays, as proposed by Ross (1997) and Ross et al. (1997), or methods based on data-driven time delays by Ikelle and Yoo (2000). Decomposition of the predicted multiples into coherent and incoherent components is an example of the second approach (Kabir, 2003), where the incoherent signal component is assumed to mostly contain diffracted multiples. In that approach, both components are simultaneously subtracted from the input data. Another example is the approach taken by Wang (2003) who improves the adaptive subtraction by introducing additional local time and phase shifts.

In this abstract, we showcase results that are obtained from the second-generation of curvelet-based primary-multiple separation algorithms. First, we briefly summarize the first-generation algorithm (see for detail Herrmann et al., 2007), followed by a brief outline of the next-generation Bayesian approach. We show that this approach has the advantage that it is less sensitive to the selection of the appropriate weights for the separation. We conclude this abstract by applying the separation method on a real dataset. For more technical details on this new Bayesian-based separation algorithm refer to another contribution by the authors to the proceedings of this conference.

Curvelet-domain primary-multiple separation

In this section, we briefly describe two curvelet-based primary multiple separation methods. For more details on the curvelet transform and the first-generation of curvelet-based separation we refer to (Herrmann et al., 2007, and the references therein).

Forward model: Both curvelet-based primary-multiple separation algorithms are based on the following forward signal model:

$$\mathbf{s} = \mathbf{s}_1 + \mathbf{s}_2 + \mathbf{n} \qquad (1)$$

with the subscript used the indicate primaries (1) and multiples (2). The symbols $\mathbf{s}$ and $\mathbf{n}$ denote the total recorded data and a white Gaussian noise term, respectively. Both approaches use SRME (see e.g. Verschuur et al., 1992) predictions for the primaries ($\check{\mathbf{s}}_1$) and multiples ($\check{\mathbf{s}}_2$) as input. The two approaches differ in how the two unknown signal components are estimated.

First-generation curvelet-based primary-multiple separation: We solve the following nonlinear weighted ℓ_1-norm optimization problem

$$\mathbf{P}_{\mathbf{w}}^l : \begin{cases} \min_{\mathbf{x}} \|\mathbf{x}\|_{\mathbf{w},1} & \text{subject to} \quad \|\mathbf{y} - \boldsymbol{A}\mathbf{x}\|_2 \le \varepsilon \\ \widetilde{\mathbf{s}}_1 = \boldsymbol{A}_1 \widetilde{\mathbf{x}}_1 \quad \text{and} \quad \widetilde{\mathbf{s}}_2 = \boldsymbol{A}_2 \widetilde{\mathbf{x}}_2 \\ \text{given:} \quad \check{\mathbf{s}}_2 \quad \text{and} \quad \mathbf{w}(\mathbf{y}, \check{\mathbf{s}}_2) \end{cases} \qquad (2)$$

where $\boldsymbol{A}_j, j = 1 \cdots 2$ are the inverse curvelet transform matrices and $\mathbf{w} = [\mathbf{w}_1, \quad \mathbf{w}_2]^T$ are the weighting vectors with strictly positive weights defined in terms of the predicted multiples, i.e., $\mathbf{w}_1 = |C_1 \cdot \boldsymbol{A}_1^T \check{\mathbf{s}}_2|$ and $\mathbf{w}_2 = |C_2 \cdot \boldsymbol{A}_2^T \check{\mathbf{s}}_1|$ with scale-dependent normalization constants $C_{1,2}$ (see Herrmann et al., 2007, for detail). The estimates for the primaries and multiples are computed from the sparsity vector that solves $\mathbf{P}_{\mathbf{w}}^l$. During the optimization, the sparsity vector is recovered by minimizing the

weighted ℓ_1 norm subject to a recovery that is within the tolerance.

This algorithm is based on the assumption that both signal components are given by a sparse superposition of curvelets, i.e.

$$\mathbf{s}_1 = \boldsymbol{A}_1 \mathbf{x}_{01} + \mathbf{n}_1 \quad \text{and} \quad \mathbf{s}_2 = \boldsymbol{A}_2 \mathbf{x}_{02} + \mathbf{n}_2 \tag{3}$$

with the vectors $\mathbf{x}_{01}$ and $\mathbf{x}_{02}$ assumed to be sparse.

$\mathbf{P}_{\mathbf{w}}^1$: can be solved using an iterative soft thresholding method with thresholds set according to the weighting vector $\mathbf{w}$. At the nth iteration, the following update is calculated

$$\mathbf{x}_j^n = T_{\lambda \cdot \mathbf{w}_j} \left(\mathbf{x}_j^n + \boldsymbol{A}_j^T \left(\mathbf{s} - \boldsymbol{A}_j \mathbf{x}_j^n - \sum_{i \neq j} \boldsymbol{A}_i \mathbf{x}_i \right) \right), \tag{4}$$

with the threshold set by the jth-component of the weighting vector and $T_\lambda(x) := \text{sgn}(x) \cdot \max(0, |x| - |\lambda|)$ the soft thresholding operator.

Second-generation curvelet-based primary-multiple separation: Unfortunately, the first-generation of primary-multiple separation is sensitive to the weighting, i.e. the emphasis of the weighing towards the primaries or multiples. Incorrect balancing for the weights yielded, after several iterations of the solver, a solution where all the signals energy could potentially end up in one (typically the primary) estimated component.

To mediate this problem, we slightly modify the nonlinear signal separation program into

$$\mathbf{P}_w^2 : \quad \begin{cases} \widetilde{\mathbf{x}} = \arg\min_{\mathbf{x}} \|\mathbf{x}_1\|_{1, \lambda_1 \cdot \mathbf{w}_1} + \|\mathbf{x}_2\|_{1, \lambda_2 \cdot \mathbf{w}_2} + \\ \|\check{\mathbf{s}}_2 - \boldsymbol{A}_2 \mathbf{x}_2\|_2^2 + \eta \|\check{\mathbf{s}}_1 + \check{\mathbf{s}}_2 - \boldsymbol{A}_1 \mathbf{x}_1 - \boldsymbol{A}_2 \mathbf{x}_2\|_2^2 \\ \widetilde{\mathbf{s}}_1 = \boldsymbol{A}_1 \widetilde{\mathbf{x}}_1 \quad \text{and} \quad \widetilde{\mathbf{s}}_2 = \boldsymbol{A}_2 \widetilde{\mathbf{x}}_2. \end{cases}$$

Again the $\check{\mathbf{s}}_{1,2}$ represent the SRME-predicted primaries and multiples, $\boldsymbol{A}_{1,2}$ the inverse discrete curvelet transforms, $\mathbf{x} = [\mathbf{x}_1, \mathbf{x}_2]^T$ the unknown curvelet vector for the primaries ($\mathbf{x}_1$) and multiples ($\mathbf{x}_2$). The $\lambda_{1,2}$ and η are control parameters determining the emphasis on the data misfit, the confidence in the multiple prediction, and the noise level. The estimates for the separated signal components is obtained by the inverse curvelet transform of the $\widetilde{\mathbf{x}}_{1,2}$ that minimize above nonlinear program.

This weighted nonlinear sparsity promoting program ($\boldsymbol{P}_w^2$) attempts to find the sparsest sets of curvelet coefficients for the primaries and multiples that fit the predicted multiples **and** the total data. This program is different from $\boldsymbol{P}_w^1$, where the two sparsest sets of coefficients are sought that fit the total data. The additional ℓ_2-penalty term ensures that the coefficients for the multiples fit the SRME-predicted multiples.

The parameters λ_1 ands λ_2 and η control the emphasis on the sparsity prior versus the data misfit. The parameter η expresses the confidence in the total data compared to the prediction for the multiples. The λ_1, λ_2 determine the level of sparsity for the primaries and multiples, respectively.

The above nonlinear optimization problem can be solved by an iterative thresholding procedure. After n iterations, the estimates for the two seperated signal components are given by

$$\begin{aligned} \mathbf{x}_1^{n+1} &= \boldsymbol{T}_{\hat{\lambda}_1 \cdot \mathbf{w}_1} \left[\mathbf{x}_1^n + \boldsymbol{A}^T \left(\check{\mathbf{s}}_1 + \check{\mathbf{s}}_2 - \boldsymbol{A} \mathbf{x}_1^n - \boldsymbol{A} \mathbf{x}_2^n \right) \right] \\ &\qquad\qquad\qquad\qquad\qquad\qquad\qquad\qquad\qquad (5) \\ \mathbf{x}_2^{n+1} &= \boldsymbol{T}_{\hat{\lambda}_2 \cdot \mathbf{w}_2} \left[\mathbf{x}_2^n + \boldsymbol{A}^T \left(\check{\mathbf{s}}_2 - \boldsymbol{A} \mathbf{x}_2^n \right) + \hat{\eta} \boldsymbol{A}^T \left(\check{\mathbf{s}}_1 - \boldsymbol{A} \mathbf{x}_1 \right) \right] \end{aligned}$$

with $\hat{\lambda}_1 = \frac{\lambda_1}{2(1+\eta)}, \hat{\lambda}_2 = \frac{\lambda_2}{2\eta}$ and $\hat{\eta} = \frac{\eta}{\eta+1}$.

APPLICATION TO THE SAGA DATA SET

The proposed algorithm is tested on the SAGA dataset (see e.g. Verschuur et al., 1992, for a detailed description of this dataset), consisting of 128 sources and receivers and 1024 time samples. The 3-D discrete curvelet transform with wrapping was used (Ying et al., 2005) using 32 angles at the finest scale. The SRME results (Fig. 2) were obtained using a spatially varying matched filter. The single threshold results (Fig. 3) were obtained by running Eq. 4 with only one iteration and $C_1 = 1$. The second generation results were obtained for 7 iterations with $\eta = 2.0$, $\lambda_1 = 3.0$ and $\lambda_2 = 3.0$. Both curvelet-based results (Figs 3 and 4) contain less high-frequency clutter compared to the SRME result in Fig. 2 while the solution of $\boldsymbol{P}_w^2$ leads to an improved multiple removal compared to the single thresholded result (cf. Figs 3,4).

DISCUSSION AND CONCLUSIONS

By virtue of their compression capabilities, localization, multiscale, and multi-angular nature curvelets represent the ideal domain for primary-multiple separation. Not only does the curvelet construction allow for a separation based on differences in these curvelet attributes but their compression also allows for a sparsity promoting formulation of the primary-multiple separation problem. In addition, the compression reduces the probability of having large entries for each signal component at the same location in the curvelet vector. Moreover, the curvelet's multi-angular parameterization helps the separation, even for conflicting dips and erroneous predictions. The reformulation of the separation problem resolved an earlier shortcoming by adding an additional constraint controlling the misfit between the estimated and SRME-predicted multiples. The results of applying this method to real data show a clear improvement over SRME-predicted primaries and over the earlier generation of curvelet-based primary-multiple separation.

Curvelet-based primary-multiple separation

Figure 1: Total data SAGA data.
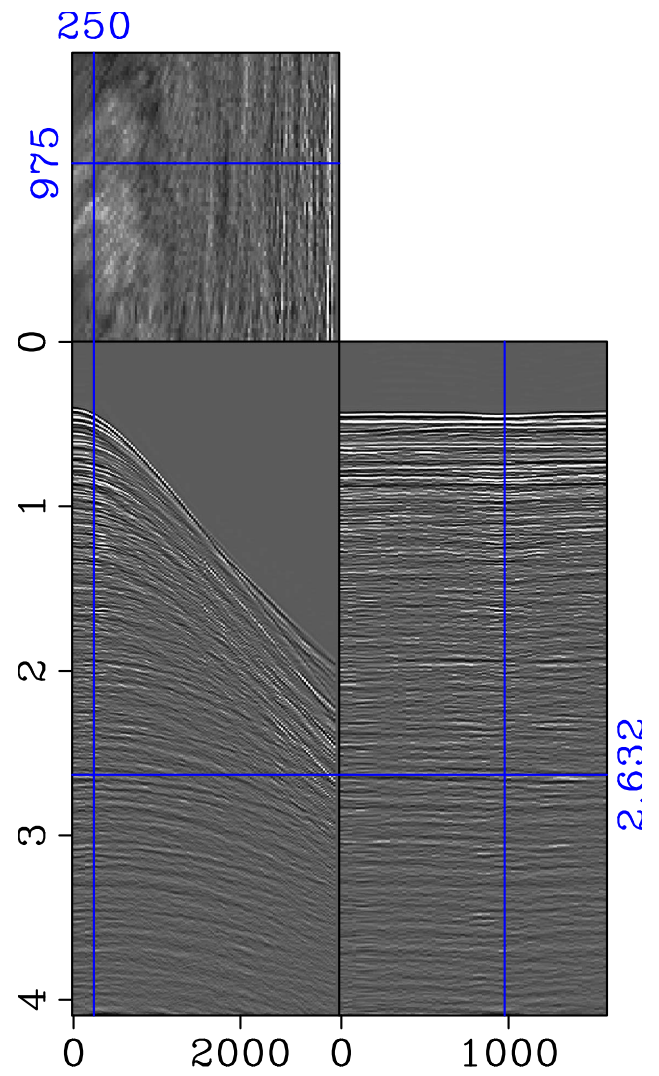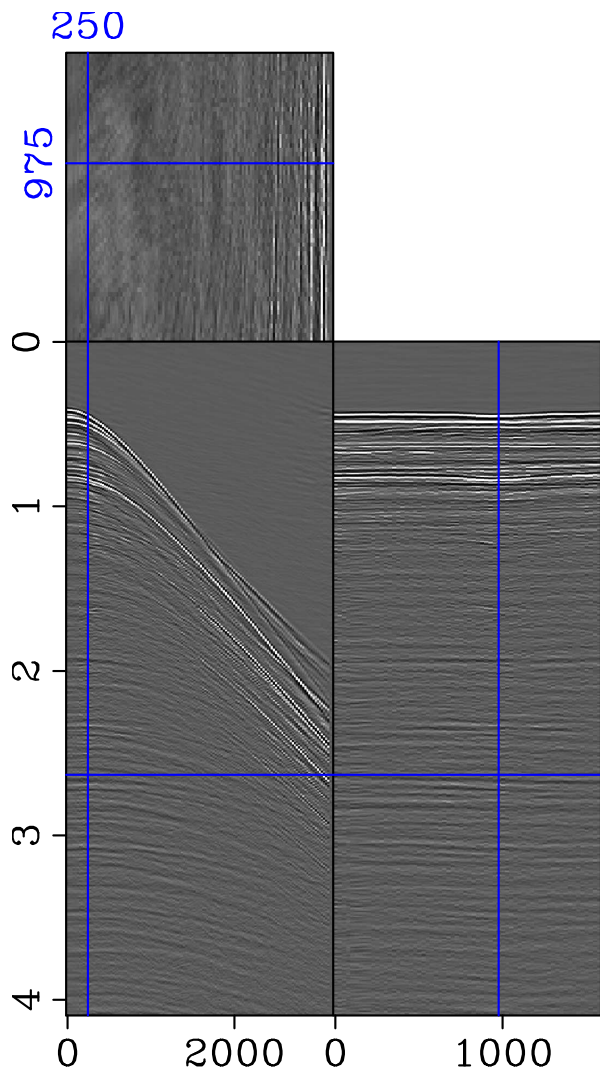

Figure 2: SRME-predicted primaries.

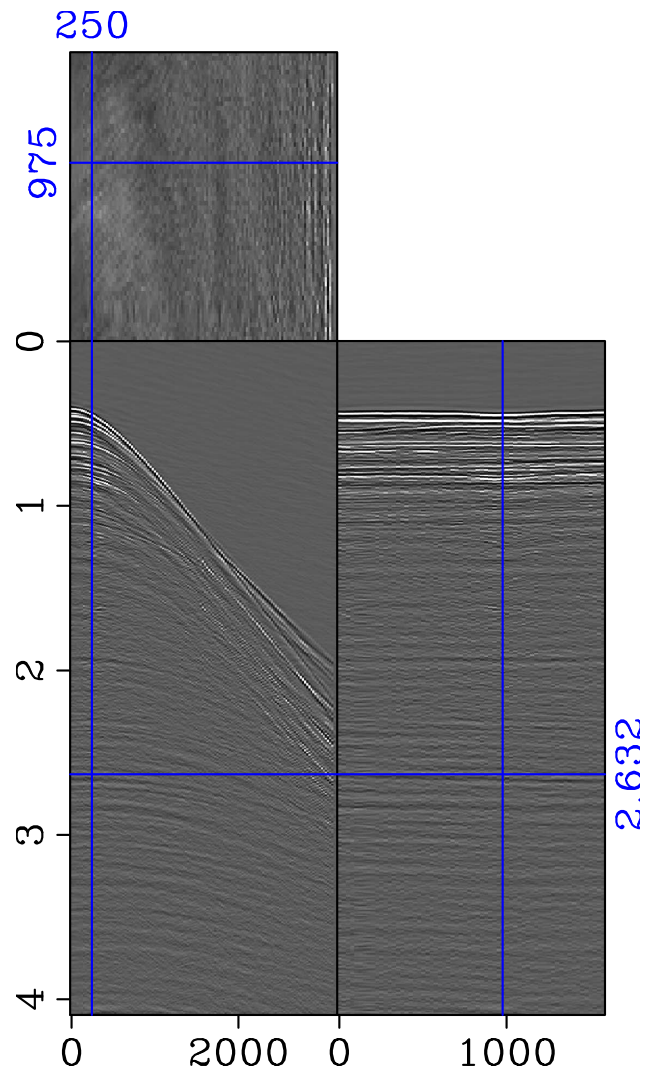Figure 3: Estimated primaries with single thresholding.

Figure 4: Estimated primaries according to P_w^2.

Curvelet-based primary-multiple separation

REFERENCES

Berkhout, A. J. and D. J. Verschuur, 1997, Estimation of multiple scattering by iterative inversion, part I: theoretical considerations: Geophysics, **62**, 1586–1595.

Berryhill, J. R. and Y. C. Kim, 1986, Deep-water peg legs and multiples: Emulation and suppression: Geophysics, **51**, 2177–2184.

Chen, J., E. Baysal, and O. Yilmaz, 2004, Weighted subtraction for diffracted multiple attenuation: 74th Ann. Internat. Mtg., SEG, Expanded Abstracts, 1329–1332, Soc. Expl. Geophys., Expanded abstracts.

Coates, R. T. and A. B. Weglein, 1996, Internal multiple attenuation using inverse scattering: Results from prestack 1 and 2-D acoustic and elastic synthetics: 66th Ann. Internat. Mtg., SEG, Expanded Abstracts, 1522–1525, Soc. Expl. Geophys., Expanded abstracts.

Fokkema, J. T. and P. M. van den Berg, 1993, Seismic applications of acoustic reciprocity: Elsevier.

Herrmann, F. J., U. Boeniger, and D.-J. E. Verschuur, 2007, Nonlinear primary-multiple separation with directional curvelet frames: Geoph. J. Int. To appear.

Ikelle, L., G. Roberts, and A. Weglein, 1997, Source signature estimation based on the removal of first-order multiples: Geophysics, **62**, 1904–1920.

Ikelle, L. T. and S. Yoo, 2000, An analysis of 2D and 3D inverse scattering multiple attenuation: 70th Ann. Internat. Mtg., SEG, Expanded Abstracts, 1973–1976, Soc. Expl. Geophys., Expanded abstracts.

Kabir, M. M. N., 2003, Weighted subtraction for diffracted multiple attenuation: 73rd Ann. Internat. Mtg., SEG, Expanded Abstracts, 1941–1944, Soc. Expl. Geophys., Expanded abstracts.

Lokshtanov, D., 1999, Multiple suppression by data-consistent deconvolution: The Leading Edge, **18**, 115–119.

Ross, W. S., 1997, Multiple suppression: beyond 2-D. part I: theory: 67th Ann. Internat. Mtg., Expanded Abstracts, 1387–1390, Soc. Expl. Geophys., Expanded abstracts.

Ross, W. S., Y. Yu, and F. A. Gasparotto, 1997, Multiple suppression: beyond 2-D. part II: application to subsalt multiples: 67th Ann. Internat. Mtg., Expanded Abstracts, 1391–1394, Soc. Expl. Geophys., Expanded abstracts.

Verschuur, D. J., 2006, Seismic multiple removal techniques: past, present and future: EAGE publications b.v. edition.

Verschuur, D. J. and A. J. Berkhout, 1997, Estimation of multiple scattering by iterative inversion, part II: practical aspects and examples: Geophysics, **62**, 1596–1611.

Verschuur, D. J., A. J. Berkhout, and C. P. A. Wapenaar, 1992, Adaptive surface-related multiple elimination: Geophysics, **57**, 1166–1177.

Wang, Y., 2003, Multiple subtraction using an expanded multichannel matching filter: Geophysics, **68**, 346–354.

Weglein, A. B., F. A. Carvalho, and P. M. Stolt, 1997, An iverse scattering series method for attenuating multiples in seismic reflection data: Geophysics, **62**, 1975–1989.

Wiggins, J. W., 1988, Attenuation of complex water-bottom multiples by wave-equation-based prediction and subtraction: Geophysics, **53**, 1527–1539.

Ying, L., L. Demanet, and E. J. Candés, 2005, 3D discrete curvelet transform: Wavelets XI, Expanded Abstracts, 591413, SPIE.